

Decay of ^{100}Sr and a “pairing-free” $K^\pi=1^+$ rotational band in odd-odd ^{100}Y

F. K. Wohn, John C. Hill, and J. A. Winger
Ames Laboratory and Iowa State University, Ames, Iowa 50011

R. F. Petry and J. D. Goulden
University of Oklahoma, Norman, Oklahoma 73019

R. L. Gill, A. Piotrowski,* and H. Mach†
Brookhaven National Laboratory, Upton, New York 11973
 (Received 20 April 1987)

The decay of ^{100}Sr (193 ms) to the low-spin ^{100}Y isomer (735 ms) was studied from mass-separated activity produced in thermal neutron fission of ^{235}U . γ singles and γ - γ coincidence measurements resulted in the placement of 67 γ transitions in a decay scheme with 26 levels below 2 Mev. The multipolarities of low-energy transitions were determined from internal conversion electron measurements. $\log ft$ values were deduced using an absolute γ -ray intensity determination for the $A=100$ decay chain. The 1^+ levels in ^{100}Y at 10.70 and 974.61 keV each receive $\sim 40\%$ of the β feeding from ^{100}Sr . A $K^\pi=1^+$ rotational band (with 1^+ , 2^+ , and 3^+ levels at 10.70, 76.15, and 172.03 keV) is proposed which can be characterized as a nearly “pairing-free” band. Other levels in ^{100}Y are discussed in terms of two-quasiparticle Nilsson orbitals.

I. INTRODUCTION

Neutron-rich nuclei with $Z \simeq 40$ and $A \simeq 100$ comprise a new region of deformation. Many of the properties of $A \simeq 100$ nuclei have been revealed during the last decade, primarily by means of studies done at ISOL (isotope separator on-line) facilities. Recent reviews of these properties (Refs. 1–4 and the references therein) describe characteristics of odd-odd and odd- A nuclei as well as the more completely studied even-even nuclei. Briefly, this region of nuclei exhibits three unusual characteristics: (1) an extremely abrupt onset of deformation at $N \simeq 60$, (2) coexistence of nearly spherical and highly deformed shapes near $N \simeq 60$, and (3) rotational moments of inertia for deformed bands in odd-odd nuclei that are nearly equal to the rigid value.

Information about single-particle Nilsson states, deduced from the rotational bands observed in deformed odd- A nuclei,¹ strongly supports the microscopic explanation of Federman and Pittel⁵ for the unusual features of $A \simeq 100$ nuclei. They argued that strong attractive neutron-proton interactions between $g_{7/2}$ neutron and $g_{9/2}$ proton spin-orbit partners are the underlying cause of the unusual characteristics. The requirement that spin-orbit partner orbitals lie near the Fermi surface both before and after the onset of deformation is satisfied since the onset occurs for $Z \simeq 40$ and $N \simeq 60$. For these nucleon numbers the Nilsson states $\pi_{1/2}^5[422]$ for odd- Z and $\nu_{3/2}^3[411]$ for odd- N , which are deformed “partner” orbitals, have been identified as low-lying bandheads in odd- A deformed nuclei.^{1–4}

Odd-odd nuclei such as Y and Nb in the $A \simeq 100$ region with $N > 60$ are expected to be quite deformed, particularly for two-quasiparticle states with a $\frac{5}{2}[422]$ pro-

ton coupled to a $\frac{3}{2}[411]$ neutron.^{2,4} A $K^\pi=1^+$ band formed from such a neutron-proton coupling should be strongly fed in the β^- decay of the 0^+ even-even parent nucleus. In Ref. 4 we presented preliminary data on the deformed odd-odd $^{100,102}\text{Y}$ and $^{102,104}\text{Nb}$ nuclei and proposed that four $K^\pi=1^+$ bands (one in each nucleus) are nearly “pairing-free” bands. In Ref. 3 we presented the decay scheme for the decay of ^{102}Sr to ^{102}Y and summarized the changes in the structure of Y nuclei around $N=60$. In the present paper we present our detailed decay scheme for the decay of ^{100}Sr and compare it with previous information^{6–9} on the decay of ^{100}Sr . The present ^{100}Sr decay scheme establishes, via $\log ft$ assignments that could not be made from our preliminary data, the $K^\pi=1^+$ bandhead in ^{100}Y . Possible two-quasiparticle assignments of other levels in ^{100}Y are also discussed.

II. EXPERIMENTAL METHODS AND RESULTS

A. Source preparation

Mass-separated ^{100}Sr sources were produced at the TRISTAN mass separator facility on-line to the high flux beam reactor at Brookhaven National Laboratory. Beams of $A=100$ ions were obtained from a high-temperature Re surface ionization source containing a target of 5 g of enriched ^{235}U which was exposed to a thermal neutron flux of 3×10^{10} n/cm²s (Ref. 10). At the ion source temperatures employed, Sr was the dominant component of the $A=100$ ion beam and only trace amounts of Rb were present. As was discussed in our study³ of the decay of ^{100}Y , we were able to set an upper limit of 1% on the amount of primary Y in the beam. The mass-separated $A=100$ ion beam was deposited on

a movable aluminum-coated Mylar tape. There was no evidence for cross contamination from adjacent masses.

B. Half-life of ^{100}Sr

The β -decay half-lives of ^{100}Sr and ^{100}Y were determined by following the decay of intense γ rays using a Ge(Li) detector. The results of these measurements, including sample decay curves for both ^{100}Sr and ^{100}Y , were reported in Ref. 3. The half-life we obtained for ^{100}Sr was 193 ± 4 ms, where 4 ms is the rms uncertainty for several γ rays in the decay of ^{100}Sr . Our result is slightly smaller than the values 214 ± 8 ms (based on γ rays)⁸ and 201 ± 4 ms (based on delayed neutrons).⁹

C. Internal conversion electron measurements

Spectra were obtained using a Si(Li) detector of 200 mm² area, 3 mm depletion depth, and 1.6-keV resolution (FWHM) for 624-keV electrons. The Si(Li) detector, a HpGe detector, and a thin plastic scintillator viewed the activity that was deposited on an aluminized Mylar tape. The measurement point was 15 cm from the ion beam deposit point. Spectra were taken simultaneously in the Si(Li) and HpGe detectors when a coincident β signal in the plastic scintillator was present. Such β -gated spectra were free of all background activity. Both the HpGe and Si(Li) detectors were calibrated for absolute efficiency using standard sources. [Although the efficiency of the Si(Li) detector was determined primarily for electrons, it was also deduced for low-energy photons.] As on-line checks, K and L conversion electron intensities and the corresponding γ intensities for pure $E2$ transitions in even-even $A=100$ nuclei yielded conversion coefficients in excellent agreement with theoretical values.¹¹ Results of our conversion electron measurements for the ^{100}Y decay were reported in Ref. 3.

Since the data accumulation point was 15 cm away from the ion beam deposit point, decay during the transit of activity from the deposit point caused the 0.19-s ^{100}Sr activity to be relatively weak in comparison to the longer-lived activities of ^{100}Y , ^{100}Zr , ^{100}Nb , etc. The lower part of Fig. 1 shows a Si(Li) spectrum obtained under these conditions. The upper part of Fig. 1 shows a γ spectrum obtained at the point of deposit of the ion beam using a high-resolution planar HpGe detector. In this HpGe spectrum the 0.19-s ^{100}Sr γ rays are enhanced. Since the intense 65-keV transition is the only ^{100}Sr transition cleanly resolved from other peaks in the Si(Li) spectrum, we were able to obtain K and L conversion coefficients only for this ^{100}Sr transition. The values we obtained were $\alpha_K = 0.53 \pm 0.05$ and $\alpha_L = 0.064 \pm 0.010$. Theoretical values¹¹ for multiplicities $E1$, $M1$, and $E2$ are, respectively, 0.325, 0.535, and 3.92 for α_K and 0.0363, 0.0622, and 0.920 for α_L . The weak 66.0-keV γ ray (discussed in Sec. II D) does not affect the $M1$ multiplicity deduced for the 65.5-keV γ ray since the 66.0-keV γ ray is only 1.6% of the 65-keV γ ray doublet intensity. The experimental α_K and α_L values are inconsistent with the possibility of $E1$ for the 65.5-keV γ ray and $E2$ for the 66.0-keV γ ray. The experi-

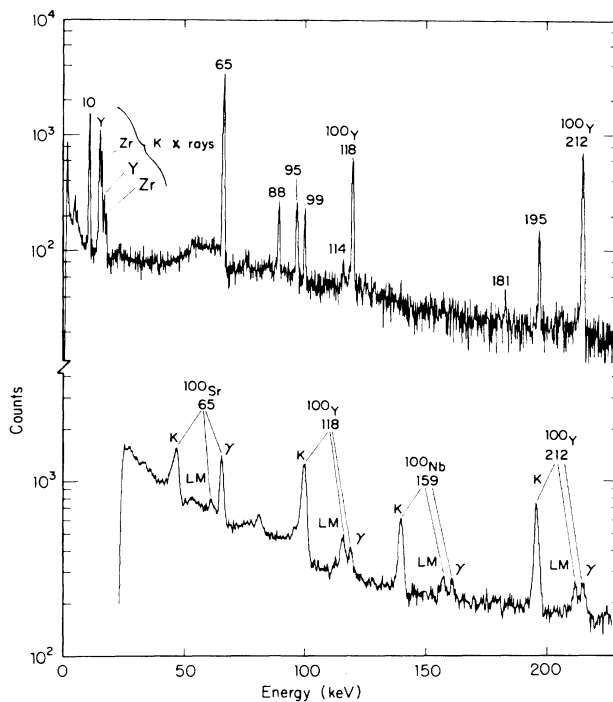


FIG. 1. Upper part: high-resolution γ -ray spectrum taken with a small planar HpGe detector with ^{100}Sr peaks labeled only by their energy. Lower part: electron spectrum taken with a Si(Li) detector with K and $L+M$ conversion electrons and γ rays labeled for the four most intense $A=100$ transitions.

mental values can be explained only with a choice of $M1$ for the 65.5-keV γ ray. (The experimental uncertainties are too large, however, to permit determination of the multipolarity of the weak 66.0-keV γ ray, for which $E2$ cannot be ruled out.) Thus our experimental values indicate essentially pure $M1$ multipolarity for the 65.5-keV transition, although we cannot exclude a small $E2$ admixture.

D. Determination of γ -ray energy, intensity, and coincidence relationships

Several γ singles and γ - γ coincidence measurements were made for mass-separated $A=100$ nuclei. Both types of spectra were taken with time cycles (i.e., beam deposit time and data accumulation time) chosen to enhance either the 0.19-s ^{100}Sr or the 0.74-s ^{100}Y activity. Both singles and β -gated singles spectra were obtained with several Ge detectors. The various runs used for enhancement of ^{100}Y were discussed in our report³ on the decay of ^{100}Y . All γ - γ coincidence measurements for ^{100}Sr were done at the point where the $A=100$ ion beam was deposited on an aluminized Mylar tape (parent port) with two Ge detectors in 180° geometry. At the parent port a thin plastic scintillator provided the β -coincidence gate signal for β -gated spectra. These β -gated spectra were free of background γ rays. Compar-

ing β -gated and ungated singles spectra showed that there were no distortions in γ -ray intensities due to the β gate.

Figure 2 shows a γ -ray spectrum with the ^{100}Sr activity enhanced. This β -gated spectrum was obtained during the first 0.25 seconds of an 8-s gamma multiscale (GMS) cycle that consisted of 32 time-sequential β -gated spectra, each of 0.25-s duration. The first 16 spectra were taken while the ion beam was being deposited and the second 16 with the beam deflected. Consequently, the 0.19-s ^{100}Sr γ rays are enhanced in Fig. 2 relative to the longer-lived members of the $A = 100$ decay chain. The more intense ^{100}Sr γ rays were distinguished from γ rays belonging to other $A = 100$ nuclei and their energies and intensities determined from these GMS spectra.

The upper part of Fig. 1 shows the low-energy portion of a spectrum obtained with a small planar HpGe detector. The 10.68-keV γ ray was cleanly resolved from all x rays. In particular, due to the good resolution (0.47 keV FWHM at 10 keV), an upper limit of 1% (of the 10.68-keV intensity) could be set on the 9.88-keV Ge "escape peak" x rays. The GMS data (consisting of nine spectra, each of 0.1-s duration) showed that the 10.68-keV γ ray decayed at the same rate as the ^{100}Sr γ rays and ^{100}Y K x rays. Energies and relative intensities of the low-energy ^{100}Sr γ rays were in excellent agreement with values obtained earlier using larger-volume Ge detectors.

Absolute γ -ray intensities were determined using an equilibrium $A = 100$ Ge spectrum and assuming only ions of Rb and Sr were present in the $A = 100$ beam. A saturation spectrum was obtained in which Sr, Y, and Zr activities were in equilibrium with the ion-beam deposition rate. Details of this run are given in Ref. 3. Briefly, by comparing ^{100}Y rays to ^{100}Zr γ rays whose absolute intensities have been published, we determined that there is no β feeding to the ground state of ^{100}Zr in the decay of the low-spin isomer of ^{100}Y (Ref. 3). The same saturation spectrum was used in the present study to determine absolute intensities of ^{100}Sr γ rays.

Figure 3 shows the low-energy portions of four γ - γ coincidence spectra. These spectra, which are selected to illustrate the existence of a 95.9-keV doublet in the ^{100}Sr decay, are discussed in Sec. III. In order to establish the ^{100}Sr decay scheme, it was necessary to determine energies and relative intensities of coincident γ rays in several selected gates because, in the GMS spectra, many ^{100}Sr γ rays were either not resolved from other transitions in the $A = 100$ decay chain or were so weak that they could only be observed in coincidence spectra.

Compton-scattered peaks, such as those in Fig. 3 labeled 212 CS (for a 212-keV Compton-scattered γ ray), can occur in γ - γ coincidence spectra. In a coincidence spectrum for a γ -ray gate of energy E_g , CS peaks are observed when an intense γ ray of energy E_γ is Compton

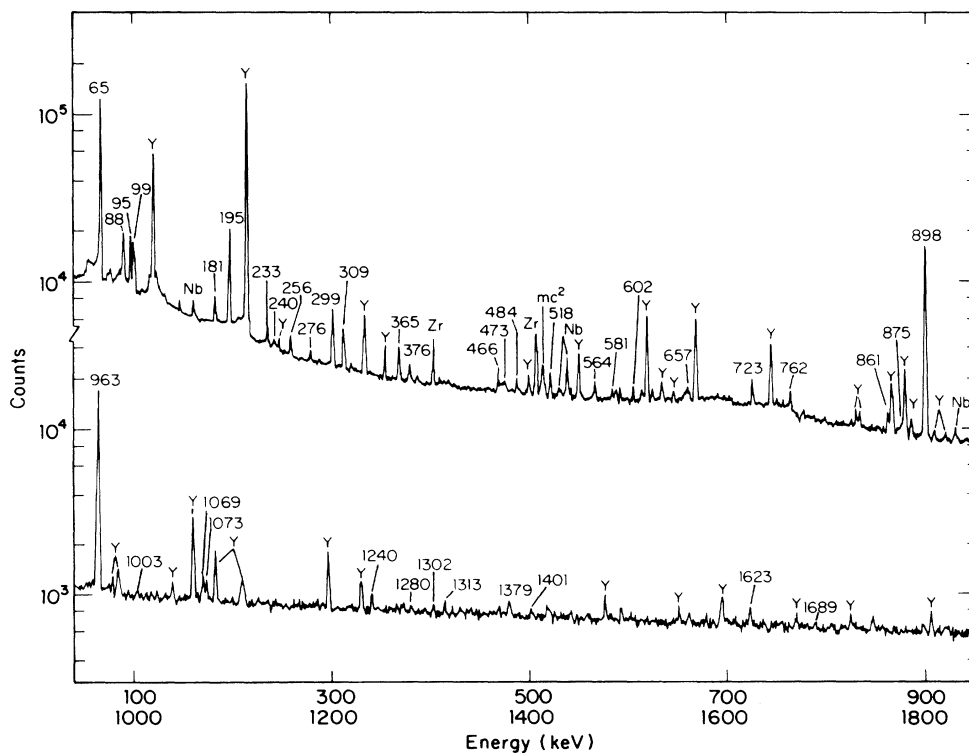


FIG. 2. γ -ray spectrum with enhanced ^{100}Sr activity. Selected ^{100}Sr peaks are labeled by energy and other $A = 100$ peaks are labeled by their element symbol Y, Zr, Nb.

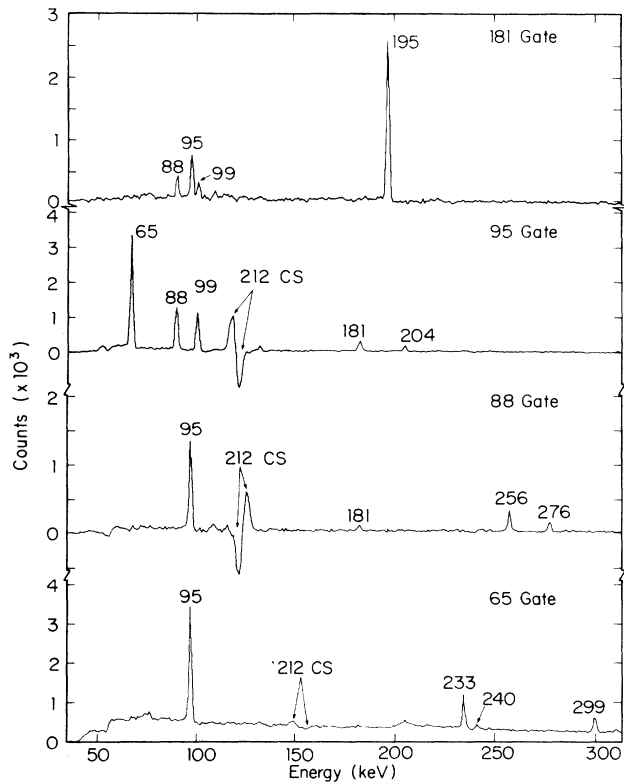


FIG. 3. Low-energy portions of coincidence spectra for four gates with ^{100}Sr γ rays labeled by energy. The bipolar peaks in the 65-, 88-, and 95-keV gates, due to Compton-scattered photons from the intense 212.6-keV γ ray in ^{100}Y , are discussed in Sec. II D.

scattered from one detector into another, leaving energy E_g in the gated detector and energy $E_\gamma - E_g$ in the other detector. In a difference spectrum (i.e., peak minus background), they appear as "bipolar" peaks. In Fig. 3, the 88- and 95-keV gated spectra show bipolar peaks with energies of ≈ 125 and ≈ 117 keV, respectively. (Since the same background gate was used for both peak gates, the negative parts of both bipolar peaks occur at ≈ 121 keV.) The likelihood of observing such bipolar peaks for any γ ray can be predicted from the relative intensities of the true γ rays and the probability of Compton scattering. In the 88- and 95-keV gates the CS peaks are relatively large since their energies are close to the 116.0-keV energy for the Compton backscattering (180°) of a 212.6-keV γ ray. As is discussed in Sec. III B, such CS peaks may not have been recognized as such in a previous ^{100}Sr decay study.⁷

Table I gives energies, intensities, level placements, and coincidence relationships of γ transitions in the ^{100}Sr decay. Energy uncertainties are due to statistical factors and system nonlinearities. Uncertainties in γ -ray intensities are due to statistical factors and uncertainties in the photopeak efficiency curves for the detectors used. Values for the 10.7-keV γ ray came from the small planar HpGe detector. For other γ rays below 200 keV, the values listed are weighted averages of spectra from

three detectors: a small planar HpGe, a moderate-size HpGe, and a large Ge(Li). For γ rays above 200 keV, only the latter two detectors were used. Due to the close detector geometry, the effects of single-detector coincidence summing were not negligible, requiring corrections to be made for both summing-in and summing-out effects. Such summing corrections were negligible only for the Si(Li) and small planar HpGe detectors.

Several transitions listed in Table I were established by analysis of selected coincidence spectra. Once the placement of each component of the unresolved doublets at 65, 95, and 299 keV had been deduced via its γ - γ coincidence relationships, accurate energies and intensities were found by fitting the peaks in the appropriate coincidence spectra. The energy and relative intensity of the 66.0-keV transition were determined from three gates: 299, 309, and 484 keV. Analysis of singles and coincidence spectra showed the 66.0-keV component to have $(1.6 \pm 0.2)\%$ and the 65.5-keV component to have $(98.4 \pm 0.7)\%$ of the intensity of the 65-keV doublet. (For this reason the 66.0-keV component does not affect the $M1$ multipolarity deduced for the 65.5-keV transition.) For the 299-keV doublet, the 466- and 518-keV gates determined the 299.0-keV component and the 65- and 484-keV gates determined the 299.7-keV component. In all cases there was excellent agreement between the results for a given γ ray from the different gates. As Table I reveals, however, both γ rays in the 95.9-keV doublet have, within experimental uncertainties, the same energy. This explains why the 95-keV peak does not appear to be a doublet in the high-resolution HpGe spectrum of Fig. 1.

III. DECAY SCHEME FOR ^{100}Sr

The level scheme for ^{100}Y from the decay of ^{100}Sr is shown in Fig. 4. It is based on γ -ray singles and coincidence measurements. Placements of individual γ rays are given in Table I. The β branching ratios and $\log ft$ values were determined from transition intensity balances. A Q_β value of 7090 ± 150 keV, reported by Pahlmann *et al.*,⁶ was used. The multiplicities of the intense transitions at 10.7 and 65.5 keV were found experimentally to be $E1$ and $M1$, respectively, as indicated in Fig. 4. Our conversion electron measurement (discussed in Sec. II C) showed that the 65.5-keV transition was essentially pure $M1$. The $E1$ multiplicity of the 10.7-keV transition was deduced as explained in the following.

At 10.7 keV, the total conversion coefficients for Y are 8.71, 15.77, and 6171 for $E1$, $M1$, and $E2$, respectively.¹¹ The transition's multipolarity thus strongly affects the total branching (β , γ , and e^-) to the ground state of ^{100}Y . Using our decay scheme and absolute γ -ray intensities, the total branching to the ^{100}Y ground state due to γ rays and conversion electrons is 103 ± 4 per 100 decays of ^{100}Sr with $E1$ multipolarity for the 10.7-keV transition. A choice of $M1$ multipolarity, however, leads to the impossible value of 173 ± 7 per 100 decays of ^{100}Sr . Any multipolarity for the 10.7-keV γ ray other than $E1$

TABLE I. γ transitions observed in decay of ^{100}Sr .

E_γ (keV)	I_γ ^a	Placement (keV)		Coincident γ rays (keV) ^b
10.68 (3)	44 (4)	10.70	0	
65.46 (3)	69 (5)	76.15	10.70	95,(107),(204),233,240,299.7, (311),376,407,466,(518),(526), (562),622,(655),657,(873),898, 969,1069,1073,(1240),1302, 1313,1623
66.0 (6) ^c	1.11 (15)	376.04	309.86	299.309,484,(518),964,1003
88.50 (3)	6.4 (3)	99.16	10.70	95,181,256,276,(376),384,505, 518,762,875,(964),(1241),1280
95.91 (4) ^d	3.68 (25)	194.98	99.16	88,99,(107),181,(288),518,564, 581,(602),665,(1069),(1183)
95.94 (4) ^d	3.13 (16)	172.03	76.15	65,204,311,(376),526,562,655, 873,(1240)
99.20 (3)	5.75 (25)	99.16	0	95,181,256,276,(376),384,505, 518,762,875,(964),(1241),1280
107.43 (11) ^d	0.48 (7)	483.57	376.04	(65),(95),(181),(299),365,376, (518)
114.86 (5)	0.88 (6)	309.86	194.98	195,466,(550),602,(964),1069
127.65 (11) ^c	0.13 (2)	483.57	355.75	256
181.17 (3)	2.46 (12)	376.04	194.98	88,95,99,(107),195,473,484, (518),964,1003
195.01 (3)	15.9 (7)	194.98	0	114,181,288,(473),(466),484, 518,564,581,602,633,665,951, 964,1003,1069,1183
204.11 (8)	0.26 (4)	376.04	172.03	(65),95
233.77 (4)	1.84 (10)	309.86	76.15	65,466,518,539,564,602,1069
240.64 (8)	0.77 (7)	1389.97	1149.40	65
256.63 (4)	2.01 (10)	355.75	99.16	88,99,127,(376),505,518
276.90 (6)	0.94 (9)	376.04	99.16	88,99,473,484,(518),964,1003
285.11 (8)	0.39 (6)	1146.33	861.19	762
288.7 (3) ^c	0.04 (1)	483.57	194.98	(95),195
299.03 (5) ^d	5.6 (4)	309.86	10.70	66,(107),(376),466,484,518, 539,(550),564,602,(964),1069
299.70 (6) ^c	1.10 (7)	376.04	76.15	65
309.68 (6) ^d	3.75 (22)	309.86	0	66,(376),466,(484),518,539, (550),564,602,(964),1069
311.62 (19) ^c	0.28 (6)	483.57	172.03	(65),95
365.31 (4)	3.22 (17)	376.04	10.70	107,(376),473,484,(518),964, 1003
376.96 (7)	1.58 (11)	860.60	483.57	65,(88),(95),(99),107,(256), (299),(309),(365),384,407,518
384.55 (14) ^d	0.42 (7)	483.57	99.16	88,99,376,518
407.43 (8)	0.52 (6)	483.57	76.15	65,376,518
466.46 (6)	2.61 (17)	776.25	309.86	65,114,(195),233,299,309,564, 602
473.33 (15) ^d	0.80 (12)	849.47	376.04	181,(195),276,365
484.77 (8)	1.41 (12)	860.60	376.04	66,181,195,276,299,(309),365, 518
505.09 (8) ^c	1.04 (9)	860.60	355.75	88,99,256,518
518.67 (6)	3.07 (17)	1379.17	860.60	(66),88,95,99,(107),(181),195, 233,256,(276),299,309,(365), 376,384,407,484,505,(550),665
526.72 (8) ^c	0.36 (6)	698.71	172.03	(65),95
539.64 (8)	0.71 (9)	849.47	309.86	233,299,309
550.45 (19) ^c	0.33 (6)	860.60	309.99	(114),(299),(309),(518)
562.08 (18) ^c	0.13 (3)	734.03	172.03	(65),95
564.56 (7) ^c	0.96 (7)	1340.73	776.25	95,195,233,299,309,466,581
581.26 (6)	1.65 (10)	776.25	194.98	95,195,564,602
602.95 (9)	2.00 (17)	1379.17	776.25	(95),114,195,233,299,309,466, 581

TABLE I. (Continued).

E_γ (keV)	I_γ ^a	Placement (keV)		Coincident γ rays (keV) ^b
622.47 (11) ^c	0.78 (9)	698.71	76.15	65
633.04 (10) ^c	0.39 (4)	827.97	194.98	195
655.87 (11) ^c	0.44 (7)	827.97	172.03	(65),95
657.84 (9)	1.01 (10)	734.03	76.15	65
665.45 (8) ^c	0.92 (9)	860.60	194.98	95,195,518
723.33 (6)	3.4 (3)	734.03	10.70	
762.06 (6)	2.9 (3)	861.19	99.16	88,99,285
861.02 (11)	1.81 (20)	861.19	0	
873.90 (14) ^c	0.44 (9)	1045.70	172.03	(65),95
875.45 (11) ^d	1.56 (17)	974.61	99.16	88,99
898.50 (4)	86 (4)	974.61	76.15	65
951.46 (16) ^c	0.38 (6)	1146.33	194.98	195
963.85 (4)	100 (4)	974.61	10.70	
964.57 (8) ^c	3.2 (3)	1340.73	376.04	66,(88),(99),(114),181,195, 276,(299),(309),365
969.02 (21) ^c	0.26 (6)	1045.70	76.15	65
1003.04 (11)	1.15 (22)	1379.17	376.04	66,181,195,276,365
1069.24 (6)	2.97 (22)	1379.17	309.86	65,(95),114,195,233,299,309
1073.31 (8)	2.04 (12)	1149.40	76.15	65
1183.90 (17) ^c	0.36 (10)	1379.17	194.98	(95),195
1240.12 (14) ^d	1.54 (16)	1412.12	172.03	(65),(95)
1241.66 (19) ^c	0.87 (15)	1340.73	99.16	(88),(99)
1280.08 (17) ^d	0.71 (17)	1379.17	99.16	88,99
1302.89 (16) ^d	0.54 (7)	1379.17	76.15	65
1313.70 (10)	1.25 (9)	1389.97	76.15	65
1379.25 (15)	1.88 (22)	1379.17	0	
1401.2 (4) ^d	0.77 (20)	1412.12	10.70	
1623.78 (10)	2.12 (13)	1700.00	76.15	65
1689.61 (25)	0.57 (16)	1700.00	10.70	

^aThese relative intensities can be converted into absolute intensities per 100 decays of ^{100}Sr by multiplying by 0.22 ± 0.01 .

^bEnergies in parentheses indicate coincidences classified as possible; all others are classified as definite. For gates set on the doublets at 65, 95, 299, 964, and 1240 keV, the partitioning of coincidences indicated in this column was determined by resolved γ -ray singlets.

^c E_γ and I_γ determined from γ - γ coincidence spectra. These γ rays were not gated unless they are one of the gated doublets listed in footnote b above.

^d E_γ and I_γ determined from an average of singles and coincidence spectra.

is inconsistent with the absolute γ -ray intensities. We thus conclude that the 10.7-keV transition is E1 and that β branching to the ^{100}Y ground state is zero (i.e., -3 ± 4 per 100 decays).

Beta branchings and $\log ft$ values are shown in Fig. 4 for the four levels whose β branches exceed 2%, within the experimental uncertainties of the γ -ray (plus conversion electron) intensity balances. The levels at 10.7 and 974 keV have large β branches and correspondingly low $\log ft$ values. For the other two levels the deduced β intensities could decrease (and the $\log ft$ values thus increase) significantly due to the cumulative effects of unobserved high-energy γ rays feeding these levels. For this reason, we are hesitant to assert that these levels are fed by allowed β transitions even though their $\log ft$ values indicate that they appear to be allowed.¹² The two levels with I_β values $> 40\%$, however, have too much β feeding to be affected in a significant way by unobserved γ rays. Their designation as 1^+ levels, based

on their very low $\log ft$ values,¹² is thus definite. The 76-keV level has both a large depopulation intensity (by the M1 65.5-keV transition) and a large population from above by γ rays, resulting in a net intensity that is zero, within the rather large experimental uncertainty of ~ 3 per 100 decays of ^{100}Sr . The experimentally deduced β branching to this level is taken to be zero, as is the deduced β branching to the ground state, although weak β branches of a few percent cannot be excluded in either case.

Reeder *et al.*⁹ determined that ^{100}Sr has a β -delayed neutron emission probability of 0.75 ± 0.08 per 100 decays of ^{100}Sr . From our γ spectra, we do not observe any of the γ rays from the decay of ^{99}Sr (Ref. 13); thus there is no evidence for β -delayed neutron branching to any excited state in ^{99}Y . However, it was not possible to place a limit lower than 0.3 per 100 decays of ^{100}Sr on a γ ray at 125.1 keV (from the first-excited state of ^{99}Y) from the γ -ray spectra. The presence of other γ rays

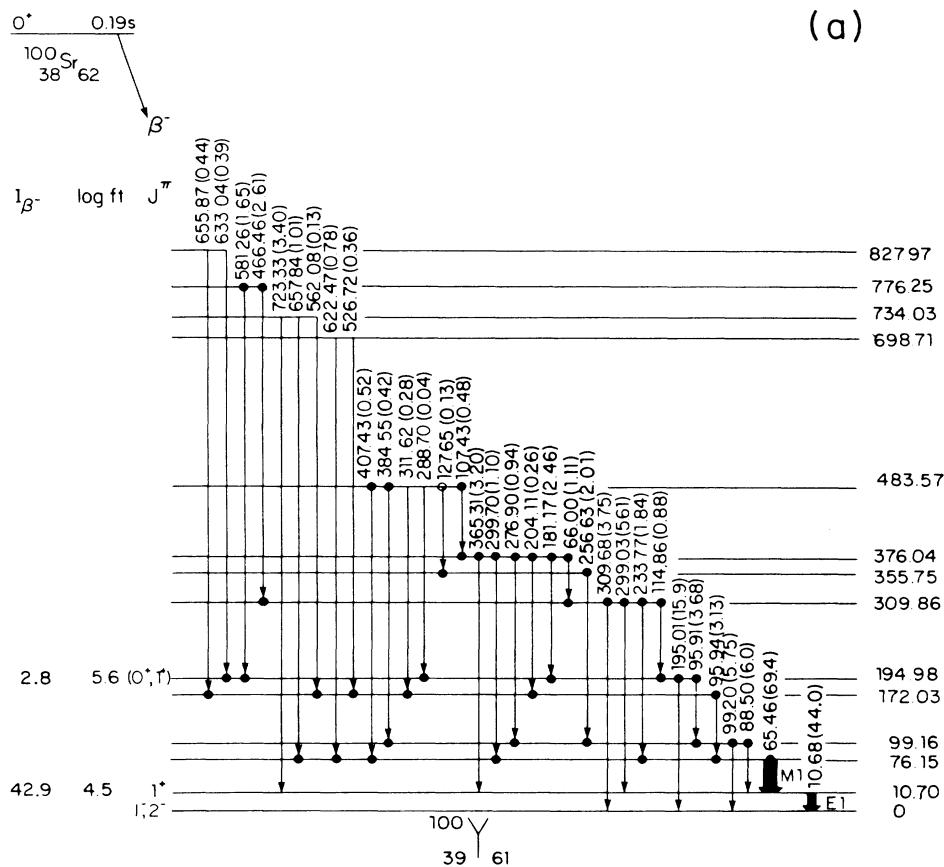


FIG. 4. Level scheme for ^{100}Y from the β decay of 0.19-s ^{100}Sr . To obtain γ -ray intensities per 100 decays of ^{100}Sr , multiply by 0.22.

near 125 keV, such as the intense ^{100}Y γ ray at 118 keV, determined the lower limit of 0.3.

A. Placement of 10.7-, 65.5-, and 95.9-keV γ rays in the ^{100}Y level scheme

The three transitions of energy 10.7, 65.5, and 95.9 keV played key roles in the determination of the ^{100}Sr decay scheme. Arguments for the placements of these γ rays are discussed in the following.

The 10.7-keV transition. Our γ - γ coincidence data revealed two pairs of γ rays (an 88.5 and 99.2 keV pair and a 299.0 and 309.7 keV pair) that differed in energy by 10.7 keV. Both γ rays in a pair had identical coincidence spectra, indicating a 10.7-keV transition. The placement of this transition was determined by additional coincidence spectra and the establishment of levels at 195, 376, and 1379 keV. The 10.68-keV γ ray was subsequently observed and its large intensity determined its placement. Including the contribution of internal conversion coefficients at 10.7 keV, this transition is the most intense one in the decay of ^{100}Sr .

The 65.5-keV transition. The placement of the 65.5-keV transition as depopulating a level at 76.1 keV was deduced from the γ - γ coincidence data. The 309-, 376-, and 1379-keV levels, each of which is well established by several coincidence relationships, led to the placement of the 65.5-keV γ ray as feeding the 10.7-keV level rather than the ground state. (It is appropriate to note here that, due to ignorance of the 10.7-keV transition, the 65.5-keV transition was placed as feeding the ground state in both Ref. 7 and in the preliminary level scheme for ^{100}Y we reported in Refs. 2 and 4.)

The 95.9-keV doublet. The recognition of a doublet at this energy also played a key role in the deduction of the ^{100}Y level scheme. Both of the 95.9-keV transitions shown in Table I (and Fig. 4) are established by γ - γ coincidence relationships with other γ rays. The coincidence gate on the 95.9-keV doublet revealed all of the coincident γ rays listed in Table I for the two components of the doublet. Since the position of each component is established by coincidences from both above and below, the possibility of only one 95.9-keV γ ray and a 23.0-keV transition can be eliminated. (Furthermore, Fig. 1 shows that no 23.0-keV γ ray is observed.)

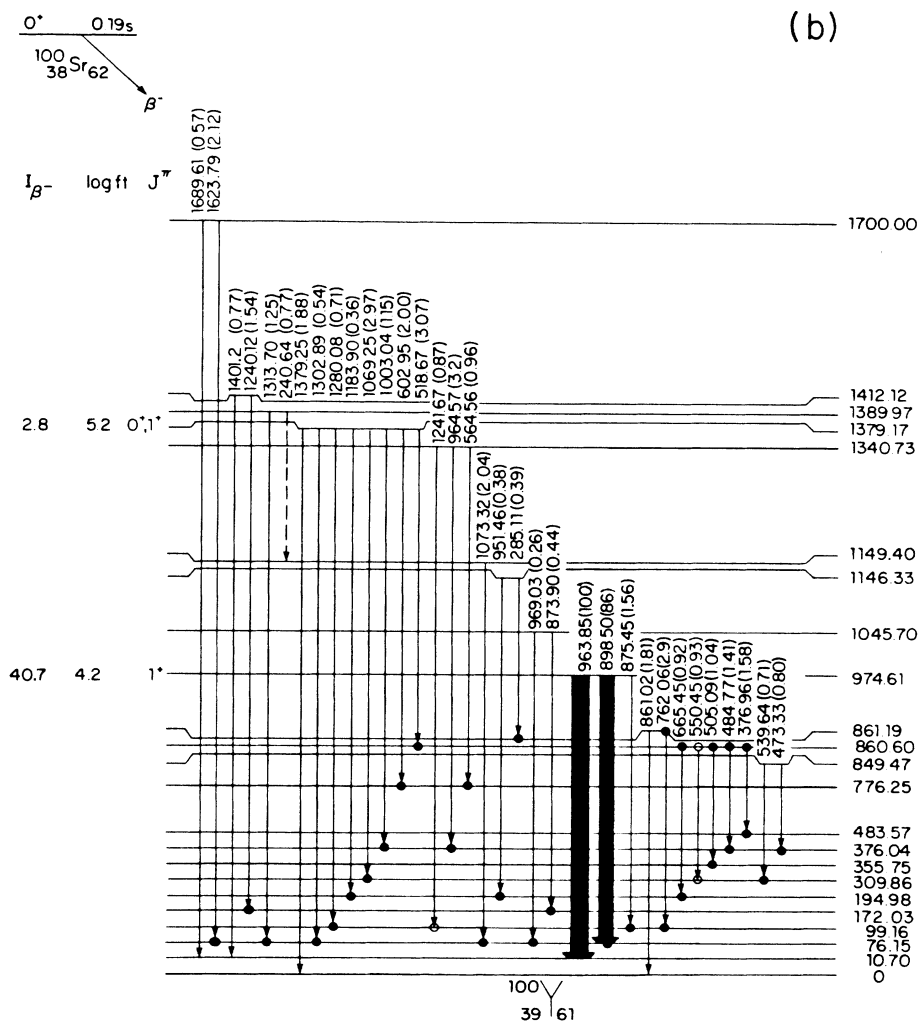


FIG. 4. (Continued).

Figure 3 illustrates some of the evidence for two γ rays at 95.9 keV. The 181-keV gate shows a 95-keV peak that has about half the intensity, compared to the 195-keV peak, as in singles. In addition, the 88- and 99-keV peaks in this gate have a total intensity equal to that of the 95-keV peak, as expected for the 95.9-keV component between the levels at 195 and 99 keV. The 88-keV gate shown in Fig. 3 allowed the intensity of this 95.9-keV γ ray to be compared to other γ rays feeding the 99-keV level. (The 99-keV gate gives the same information as the 88-keV gate and is thus not shown in Fig. 3.) The 65-keV gate shows the other component of the 95.9-keV doublet. Comparing its intensity to that of the 233.8- and 299.7-keV peaks (and also to several other peaks not shown in the low energy range of Fig. 3) helped to determine the intensity of this 95.9-keV γ ray. Analysis of relative intensities of peaks in the 95.9-keV gate confirmed the placement and relative intensity of each component of this doublet. Finally, the sum of the intensities of the two components, as determined by

coincidence spectra, agreed well with the total intensity observed in singles spectra.

B. Comparison with previous ^{100}Sr decay scheme

Our decay scheme of Fig. 4 differs significantly from the decay scheme of Münzel *et al.*⁷ In terms of the γ rays identified as belonging to the ^{100}Sr decay, the present scheme has placed 67 γ rays among 26 levels, whereas 23 γ rays were placed in 12 levels in Ref. 7. The most significant differences involve the two intense low-energy γ rays at 10.7 and 65.5 keV discussed above.

The lowest energy transition reported by Münzel *et al.*⁷ was 65.4 keV but with a much higher intensity than observed by us. Normalizing the intensity of their 964-keV γ ray to 100, they reported a 65-keV transition with an intensity of 145. Our spectra gave instead an intensity of 69 for the 65.4-keV transition. Using the small high-resolution planar HpGe detector, we carefully determined its photopeak efficiency in the energy range

10–300 keV. With the 195-keV γ -ray intensity normalized to 15.9, this measurement gave the 65-keV γ -ray intensity of 69.4. For comparison, the two larger-volume detectors we used in our γ - γ coincidence experiment gave (after summing-in and summing-out corrections were made) an average intensity of 68.5. The Si(Li) detector used for our electron measurements gave an intensity of 70.4. Thus all of our spectra, from various types of experiments using different detectors, gave the same relative intensity for the 65.4-keV γ ray.

The γ - γ coincidence results tabulated in Ref. 7, although containing far fewer γ - γ coincidences, are in essential agreement with the present work. An exception, however, concerns the six γ rays that are listed in the coincidence table of Ref. 7 at 117, 125, 174, 354, 770, and 869 keV. We found all six to be Compton-scattered peaks rather than true γ rays. (See Sec. II D.) With good coincidence statistics, they appeared in our data as well-defined bipolar peaks, as can be seen in the 88- and 95-keV gates in Fig. 3, which illustrate the false peaks at 125 and 117 keV. Each of the six false peaks included in the γ - γ coincidence table of Ref. 7 is associated with an intense γ ray in the decay of ^{100}Sr , ^{100}Y , or ^{100}Nb whose energy exceeds the gate energy by an amount that corresponds closely to Compton back-scattering. In our data, we also eliminated these six false peaks by their failure to appear in other gates that would have confirmed the placement of a true γ ray.

In Ref. 7 the extra intensity of the 65-keV γ ray led to the deduction of 1^+ for the level depopulated by this γ ray. The present study shows that this level (the 76-keV level in Fig. 4) has weak β feeding instead of 23% β feeding and a $\log ft$ of 4.9 as was deduced in Ref. 7. Therefore $\log ft$ arguments cannot be used to establish a J^π value of the 76-keV level. Our proposal⁴ that this level is 2^+ is reviewed in the next section.

IV. DISCUSSION

A. Ground-state β feeding in ^{100}Sr and ^{100}Y decays

Our experimental determination that the ^{100}Sr β branch to the ground state of ^{100}Y is essentially zero solves a puzzle that remained after our previous study³ of the decay of ^{100}Y . In Ref. 3 we determined that the ground-state β branch in the decay of ^{100}Y to ^{100}Zr was consistent with zero, within experimental uncertainties. At the time this fact was puzzling because we had assumed that the ground state of ^{100}Y had a J^π of 1^+ . If such were the case, then the lack of ground-state branching (supposedly 1^+ to 0^+) in the β decay of ^{100}Y to ^{100}Zr could not be understood.

With the present decay scheme for ^{100}Sr , this puzzle no longer exists, since the 10.7-keV level is the lowest 1^+ level, rather than the ground state of ^{100}Y . The absence of β feeding from ^{100}Sr to the ^{100}Y ground state is quite consistent with the absence of β feeding from ^{100}Y to the ^{100}Zr ground state. For the ^{100}Y ground state, it is not possible to assign a specific J^π , but both β decays are

consistent with 1^- or 2^- . A J^π range of 1^\pm or 2^- was determined from the β and γ decay patterns in ^{100}Y decay.³ In the present ^{100}Sr decay study, the $E1$ transition from the 10.7-keV level limits J^π to 0^- , 1^- , or 2^- . Thus, from these two ranges, only the choices 1^- or 2^- are possible for the ^{100}Y ground state.

B. The “pairing-free” $K^\pi=1^+$ band in ^{100}Y

The arguments which lead one to expect nearly “pairing-free” rotational bands (with moments of inertia nearly equal to the rigid value) for two-quasiparticle states in odd-odd deformed nuclei in the $A \simeq 100$ region have been explained in detail in Refs. 2 and 4. Briefly, the experimentally deduced moments of inertia, expressed as a fraction of those of a rigid spheroid of the same mass, were found to be unusually large (~ 0.70 for even-even and ~ 0.85 for odd- A) for deformed nuclei with $A \simeq 100$. The increase for odd- A suggests “quenching” of the residual pairing for an unpaired quasiparticle. In odd-odd nuclei, the second unpaired quasiparticle could further quench the pairing and result in a rotational band with a rigid moment of inertia. This expectation is further supported by the nearly rigid moment of inertia deduced for a high-spin band in ^{99}Y at 1655 keV which was characterized as a three-quasiparticle $K^\pi = \frac{11}{2}^+$ band.¹⁴

Figure 5 shows partial level schemes for four odd-odd nuclei. (Reference 2 gives the details on ^{102}Y and Ref. 4 gives the available information on $^{102,104}\text{Nb}$.) Compared to similar figures in Refs. 2 and 4, the energies of the ^{100}Y levels in Fig. 5 have been increased by 10.7 keV. A more significant change is that both 1^+ levels are now assigned $\log ft$ values. The low $\log ft$ value of the 10.7-

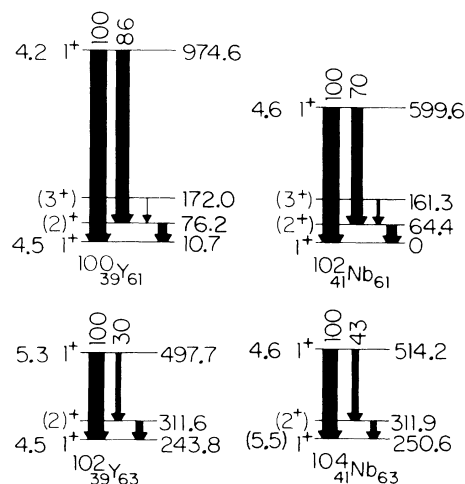


FIG. 5. Partial level schemes for odd-odd $N=61$ and $N=63$ isotones showing the $K^\pi=1^+$ rotational bands proposed earlier (Refs. 2 and 4) and revised here to correspond to the present ^{100}Sr decay scheme. $\log ft$ values are given to the left of the levels. Relative γ -ray intensities are given to the upper 1^+ levels.

keV level established the 1^+ assignment that was initially suggested by strong similarities in the level spacings and the β - and γ -decay patterns for all four odd-odd nuclei.^{2,4} (The assignments for $^{102,104}\text{Nb}$ are less firm since decay schemes for $^{102,104}\text{Zr}$ are not complete enough to allow deduction of $\log ft$ values for the lower 1^+ levels of $^{102,104}\text{Nb}$.) The lower 1^+ levels are expected to consist mainly of the two-quasiparticle configuration $\{\pi_{\frac{5}{2}}^-[422], \nu_{\frac{3}{2}}^+[411]\}$, with the upper level being mainly $\{\pi_{\frac{5}{2}}^-[422], \nu_{\frac{3}{2}}^+[422]\}$. The $\log ft$ values to the 1^+ levels are consistent with Gamow-Teller transitions, and the γ -decay patterns are consistent with unhindered $M1$ transitions which dominate over collective intraband $E2$ transitions, as the absence of 3^+ to 1^+ transitions shows.^{2,4}

C. Other two-quasiparticle Nilsson orbitals in ^{100}Y

Without the experimental signature provided by a low $\log ft$ value in β decay from a 0^+ parent, it is difficult to assign unique J^π values to other levels in ^{100}Y . Using the J^π assignments shown in Fig. 5 for the four positive parity levels in ^{100}Y , it is not possible to assign unique J^π values to other levels using the normal "rule" that only $E1$, $M1$, and $E2$ γ rays are likely to be observed. However, we can discuss the most probable choices for low-lying levels based on knowledge of Nilsson orbitals near the Fermi surface for neighboring odd- A deformed nuclei.^{1,2} The orbitals involved are $\pi_{\frac{5}{2}}^-[422]$, $\pi_{\frac{5}{2}}^-[303]$, and $\pi_{\frac{3}{2}}^+[301]$ for protons and $\nu_{\frac{3}{2}}^+[411]$, $\nu_{\frac{9}{2}}^+[404]$, $\nu_{\frac{3}{2}}^+[541]$, and $\nu_{\frac{5}{2}}^+[532]$ for neutrons. These Nilsson orbitals can be used to predict the low-lying two-quasiparticle configurations for odd-odd $A \approx 100$ nuclei. Such phenomenological calculations have been made for $^{102,104}\text{Nb}$ in Ref. 15 and for a "typical" medium-mass odd-odd nucleus in Ref. 16.

The predictions of Refs. 15 and 16 agree with the level ordering of Fig. 5, with $K^\pi=1^+ \{\pi_{\frac{5}{2}}^-[422], \nu_{\frac{3}{2}}^+[411]\}$ lower than $K^\pi=1^+ \{\pi_{\frac{5}{2}}^-[422], \nu_{\frac{3}{2}}^+[422]\}$ by ~ 0.5 MeV. Below ~ 0.3 MeV they also predict a $K^\pi=1^- \{\pi_{\frac{5}{2}}^-[303], \nu_{\frac{3}{2}}^+[411]\}$, a $K^\pi=2^- \{\pi_{\frac{5}{2}}^-[303], \nu_{\frac{9}{2}}^+[404]\}$, and $K^\pi=3^-, 0^- \{\pi_{\frac{3}{2}}^+[301], \nu_{\frac{3}{2}}^+[411]\}$. Both 0^- and 3^- are ruled out experimentally for the ^{100}Y ground state. The $2^- \{\pi_{\frac{5}{2}}^-[303], \nu_{\frac{9}{2}}^+[404]\}$ possibility is eliminated by the $E1$ multipolarity of the 10.7-keV transition, since this 2^- configuration cannot be reached by a single-particle $E1$ transition from the 1^+ level at 10.7 keV. This leaves only the 1^- choice, which has a $\pi_{\frac{5}{2}}^-[422] \rightarrow \pi_{\frac{5}{2}}^-[303]$ $E1$ transition. Thus the combination of experiment (the selectivity of the 10.7-keV $E1$ transition) and phenomenology leads to a choice of 1^- for the ^{100}Y ground state that consists of the two-quasiparticle configuration $\{\pi_{\frac{5}{2}}^-[303], \nu_{\frac{3}{2}}^+[411]\}$.

With the above prediction that the ^{100}Y ground state is a $K^\pi=1^- \{\pi_{\frac{5}{2}}^-[303], \nu_{\frac{3}{2}}^+[411]\}$ bandhead, the level at 99.2 keV can be evaluated as the 2^- member of this band. The γ -decay pattern would then have a 99.2-keV intraband $M1 + E2$ transition and an 88.5-keV interband $E1$ transition. Using transition strengths from neighbor-

ing odd- A nuclei, we predict an intraband transition that is dominated by a neutron $M1$ transition, as $(g_K - g_R)/Q_0 \sim 0$ for the $\frac{5}{2}[303]$ proton^{17,18} and $(g_K - g_R)/Q_0 \approx 0.17$ for the $\frac{3}{2}[411]$ neutron.^{18,19} With an $E1$ strength that was shown to be appropriate for $\pi_{\frac{5}{2}}^-[303] \rightarrow \pi_{\frac{5}{2}}^-[422]$ transitions in ^{99}Y and ^{103}Nb (Ref. 17), we estimate an intensity ratio (88.5 to 99.2 keV) of ~ 0.44 . This is in reasonable agreement with the experimental intensity ratio of 1.1, considering the order-of-magnitude "adjustments" typical for $E1$ strengths.²⁰ Thus, the 99.2-keV level could be the 2^- member of a tentative $1^- \{\pi_{\frac{5}{2}}^-[303], \nu_{\frac{3}{2}}^+[411]\}$ ground-state band in ^{100}Y . This 1^- band shows another similarity between the two $N=61$ isotones ^{100}Y and ^{102}Nb , since the same 1^- configuration has been associated with the lowest-energy 1^- and 2^- levels (at 20.5 and 94.0 keV) proposed for ^{102}Nb (Ref. 15).

Other possible assignments of levels to likely configurations can be considered. A band with a bandhead of $0^- \{\pi_{\frac{3}{2}}^-[303], \nu_{\frac{3}{2}}^+[411]\}$ has also been associated with low-lying levels in ^{102}Nb (Ref. 15). In ^{100}Y , the only low-lying levels that could be candidates (i.e., do not decay to either the 2^+ or 3^+ levels) for a similar 0^- bandhead are the levels at 194 and 355 keV. However, neither of these two levels has a decay pattern similar to that of the 0^- band in ^{102}Nb , and thus the similarity between ^{100}Y and ^{102}Nb does not appear to include the proposed¹⁵ 0^- band.

The 194-keV level has a $\log ft$ of 5.6, indicating that it could be fed by allowed β decay; thus it could be either 0^+ or 1^+ . (Due to the small deduced β feeding of $\approx 3\%$ and the likelihood that unobserved γ rays feed the level, there is no justification for the stronger statement that $\log ft = 5.6$ definitely shows an allowed β decay.) The 0^+ possibility would be ruled out if the 99-keV level were 2^- , as tentatively proposed above. If the 194-keV level were 1^+ , then $E1$ γ rays to the $1^- \{\pi_{\frac{5}{2}}^-[303], \nu_{\frac{3}{2}}^+[411]\}$ ground-state band should be possible, but $M1$ γ rays to the $1^+ \{\pi_{\frac{5}{2}}^-[422], \nu_{\frac{3}{2}}^+[411]\}$ band should not be possible. This γ -ray pattern would occur naturally for a $1^+ \{\pi_{\frac{5}{2}}^-[303], \nu_{\frac{3}{2}}^+[541]\}$ level at 194 keV because it would have a neutron $E1$ transition but would not have any possible single-particle $M1$ transitions. Such a 1^+ assignment for the 194-keV level, although reasonable since both Nilsson orbitals are low-lying,¹⁶ must be regarded as tentative since the multiplicities of both the β and γ transitions involved are assumed rather than established by experiment.

Although there are other levels that could correspond to additional predicted^{15,16} states, any band assignments besides the firm $K^\pi=1^+$ band at 10.7 keV are too speculative, based on current information, to be justified. This is especially true for any levels involving Nilsson orbitals (in particular neutron orbitals) for which there is a lack of experimental data on relative intraband and interband transition strengths. When such data are available, and when new conversion electron or γ - γ angular correlation data are obtained for selected transitions in ^{100}Y , then it should be possible to extend our knowledge of the band structure and the associated Nilsson orbitals in ^{100}Y .

ACKNOWLEDGMENTS

The non-BNL authors express their appreciation to the neutron-nuclear physics group at BNL for their hospitality and strong technical support. The authors ac-

knowledge the assistance in data analysis by K. Leininger and M. E. Nieland. This work was supported by the U.S. Department of Energy under Contract Nos. W-7405-eng-82, DE-AS05-79ER10495, and DE-AC07-76CH00016.

*Permanent address: Institute for Nuclear Studies, Warsaw, Poland.

†Present address: Clark University, Worcester, Massachusetts 01610.

¹*Nuclei Off the Line of Stability*, Symposium Series No. 324, edited by R. A. Meyer and D. S. Brenner (American Chemical Society, Washington, D.C., 1986). (See especially articles by Henry *et al.*, Lhersonneau *et al.*, Wohn *et al.*, and Kratz *et al.*)

²J. C. Hill, J. A. Winger, F. K. Wohn, R. F. Petry, J. D. Goulden, R. L. Gill, A. Piotrowski, and H. Mach, *Phys. Rev. C* **33**, 1727 (1986).

³F. K. Wohn, J. C. Hill, C. B. Howard, K. Sistemich, R. F. Petry, R. L. Gill, H. Mach, and A. Piotrowski, *Phys. Rev. C* **33**, 677 (1986).

⁴L. K. Peker, F. K. Wohn, J. C. Hill, and R. F. Petry, *Phys. Lett.* **169B**, 323 (1986).

⁵P. Federman and S. Pittel, *Phys. Lett.* **69B**, 385 (1977); **77B**, 29 (1978); *Phys. Rev. C* **20**, 820 (1979).

⁶B. Pahlmann, M. Graefenstedt, U. Keyser, F. Munnich, B. Pfeiffer, and H. Weikard, *Z. Phys. A* **318**, 371 (1986).

⁷J. Münzel, B. Pfeiffer, U. Stohler, G. Bewersdorf, H. Wollnik, H. Lawin, and E. Monnard, *Z. Phys. A* **321**, 515 (1985).

⁸J. Münzel, B. Pfeiffer, and H. Wollnik, *Z. Phys. A* **313**, 247

(1983).

⁹P. L. Reeder, R. A. Warner, M. D. Edmiston, R. L. Gill, and A. Piotrowski, in Ref. 1, p. 171.

¹⁰R. L. Gill and A. Piotrowski, *Nucl. Instrum. Methods* **234**, 213 (1985).

¹¹F. Rösler, H. M. Fries, K. Adler, and H. C. Pauli, *At. Data Nucl. Data Tables* **21**, 91 (1978).

¹²S. Raman and N. B. Gove, *Phys. Rev. C* **7**, 1995 (1973).

¹³R. F. Petry, H. Dejbakhsh, J. C. Hill, F. K. Wohn, M. Schmid, and R. L. Gill, *Phys. Rev. C* **31**, 621 (1985).

¹⁴R. A. Meyer, E. Monnard, J. A. Pinston, F. Schussler, I. Ragnarsson, B. Pfeiffer, H. Lawin, G. Lhersonneau, T. Seo, and K. Sistemich, *Nucl. Phys.* **A439**, 510 (1985).

¹⁵R. A. Meyer, R. W. Hoff, and K. Sistemich, Lawrence Livermore Laboratory Report UCAR 10062-84/1, 1984, pp. 6–98.

¹⁶R. A. Meyer, *Hyp. Int.* **22**, 385 (1985).

¹⁷F. K. Wohn, J. C. Hill, and R. F. Petry, *Phys. Rev. C* **31**, 634 (1985).

¹⁸F. K. Wohn, J. C. Hill, R. F. Petry, H. Dejbakhsh, Z. Berant, and R. L. Gill, *Phys. Rev. Lett.* **51**, 873 (1983).

¹⁹B. Pfeiffer, E. Monnard, J. A. Pinston, J. Münzel, P. Möller, J. Krumlinde, W. Ziegert, and K.-L. Kratz, *Z. Phys. A* **317**, 123 (1984).

²⁰C. F. Perdrisat, *Rev. Mod. Phys.* **38**, 41 (1966).